Negative Excess Shot Noise by Anyon Braiding

Byeongmok Lee, Cheolhee Han, and H.-S. Sim*
Department of Physics, Korea Advanced Institute of Science and Technology, Daejeon 34141, Korea

(Received 23 April 2018; revised manuscript received 11 March 2019; published 2 July 2019)

Anyonic fractional charges e^* have been detected by autocorrelation shot noise at a quantum point contact (QPC) between two fractional quantum Hall edges. We find that the autocorrelation noise can also show a fingerprint of Abelian anyonic fractional statistics. We predict the noise of the electrical tunneling current I at the QPC of the fractional-charge detection setup, when anyons are dilutely injected, from an additional edge biased by a voltage, to the setup in equilibrium. At large voltages, the nonequilibrium noise is *reduced* below the thermal equilibrium noise by the value $2e^*I$. This negative excess noise is opposite to the positive excess noise $2e^*I$ of the conventional fractional-charge detection and also to the usual positive autocorrelation noises of electrical currents. This is a signature of Abelian fractional statistics, resulting from the effective braiding of an anyon thermally excited at the QPC around another anyon injected from the additional edge.

DOI: 10.1103/PhysRevLett.123.016803

Abelian anyons appear in fractional quantum Hall (FQH) systems with a filling factor of $\nu = 1/(2n+1)$, $n = 1, 2, \ldots$. They obey the fractional exchange statistics [1–3]. Two anyons gain the phase $\pm\pi\nu$ when their positions are adiabatically exchanged and $\pm 2\pi\nu$ when one braids around the other. Proposals [4–20] for detecting the fractional statistics are based on interferometers or current-current cross-correlations. They involve quantities experimentally inaccessible or affected by an unintended setup change or Coulomb interaction. It will be useful to find fractional-statistics effects experimentally feasible.

Shot noise S, the zero-frequency nonequilibrium fluctuation of electrical current I, has valuable information [21]. Its Poisson value $S = 2qI$ in the tunneling regime of a quantum point contact (QPC) was used to detect the charge q of current carriers [22]. The fractional charge $e^* = \nu e$ of anyons was measured [23–29] from the ratio $S/I = 2e^*$ at a QPC between FQH edges; e is the electron charge. The Poisson value originates from the uncorrelated transfer of discrete charges. Reduction or enhancement from the value signifies effects such as resonances, diffusive scattering, Cooper pairing, etc. [21].

In this Letter, we predict unusual behavior of shot noise, originating from the Abelian fractional statistics of Laughlin anyons, in the setup [Fig. 1(a)] composed of the conventional fractional-charge detection part (edge 2, edge 3, QPC2) and an additional edge (edge 1). Anyons are dilutely injected [30–33] via QPC1 from edge 1, biased by voltage V, to the detection part in equilibrium. We find that the zero-frequency autocorrelation noise $S(V,T)$ of the tunneling current I at QPC2 is reduced below the thermal equilibrium noise $S(0,T)$ at temperature T,

$$\delta S = -2e^*I < 0 \quad \text{at } e^*V \gg k_B T. \qquad (1)$$

$\delta S \equiv S(V,T) - S(0,T)$ is the excess shot noise with respect to the thermal noise and k_B is the Boltzmann constant. The negative excess noise is unusual, since the setup has the conventional Poisson process [Fig. 1(b)] enhancing the noise; it is opposite of the positive noise $2e^*I > 0$ of the conventional fractional-charge detection [23–29]. By contrast, in the integer quantum Hall regime at

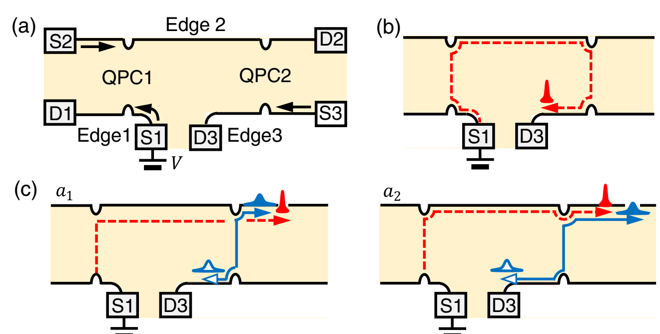

FIG. 1. (a) Setup at $\nu = (1/2n+1)$. Chiral edge channel edge i propagates (arrows) from source Si to drain Di, $i = 1, 2, 3$. S1 is biased by voltage V, while the other sources and drains are grounded. Anyon tunneling occurs at QPC1 (QPC2) between edge 2 and edge 1 (edge 3). (b) Poisson process. A particlelike anyon biased by V (narrow filled packets, dashed arrows) moves from edge 1 to D3 through tunneling at QPC1 and QPC2. (c) Interference between subprocesses a_1 and a_2. A particlelike anyon biased by V moves (dashed) from edge 1 to D2 through tunneling at QPC1. After (before) this anyon passes QPC2 along edge 2, a particle-hole pair excitation thermally occurs at QPC2 in a_1 (a_2). The particlelike anyon (wide filled packets) and the holelike anyon (wide empty) in the pair move (solid arrows) along edge 2 and edge 3, respectively. The interference between a_1 and a_2 involves braiding of the thermal anyon around the voltage-biased anyon.

$\nu = 1$, the setup shows the positive Poisson noise of $\delta S = 2eI > 0$, which cannot be extrapolated from Eq. (1) with $e^* = e/(2n+1) \to e$.

The negative excess noise results from an interference involving anyon braiding [Fig. 1(c)], which weakens thermal anyon tunneling at QPC2, reducing the noise. The reduction dominates over the enhancement by the Poisson process. Interestingly, for electrons at $\nu = 1$, the interference does not exist, as it is described by a pair of disconnected Feynman diagrams that exactly cancel each other, according to the linked cluster theorem [34]. For anyons, the cancellation is only partial, since the subdiagrams (vacuum bubbles) of one of the disconnected diagrams are linked [35] by the braiding. This type of anyon process, vacuum bubbles linked by braiding, is called topological vacuum bubbles (TVBs) [36]. Detection of the negative excess noise is experimentally feasible and will provide a signature of TVBs and the fractional statistics in the case of pristine edges (without edge reconstruction). The signature manifests itself in the leading-order contributions (in QPC tunneling strengths) to the excess noise, thanks to the dilute anyon injection at QPC1.

Excess noise.—We consider the time t average $I = \overline{I(t)}$ of tunneling current $I(t)$ at QPC2 and its zero-frequency noise $S = 2\int_{-\infty}^{\infty} dt[I(t) - I][I(0) - I]$. Employing a perturbation theory based on the chiral Luttinger liquid [37,38], Keldysh Green's functions, and Klein factors [39], we derive I and $\delta S = S(V,T) - S(0,T)$ at voltages $e^*V \gg k_B T$ in the anyon tunneling regime of $\gamma_i T^{\nu-1} \ll 1$, up to the leading order $O(\gamma_1^2\gamma_2^2)$ of tunneling strength γ_i at QPCi,

$$I \simeq e^*\gamma_1^2\gamma_2^2 f(\nu)[\cos(\pi\nu) - \cos(3\pi\nu)]V^{2\nu-1}T^{2\nu-2},$$
$$\delta S \simeq -2e^{*2}\gamma_1^2\gamma_2^2 f(\nu)[\cos(\pi\nu) - \cos(3\pi\nu)]V^{2\nu-1}T^{2\nu-2}. \quad (2)$$

This gives Eq. (1) [40,41]. Notice that $I > 0$, but $\delta S < 0$. The factors having $\pi\nu$ originate from anyon braiding.

The current I and excess noise δS are linked to measurable quantities. I equals the average current $I_3 = \overline{I_3(t)}$ at D3, as only S1 is biased. δS is obtained [41] by

$$\delta S = S_3(V,T) - 4k_B T \frac{\partial I_3(V,T,V_3)}{\partial V_3}\bigg|_{V_3=0} - \left(S_3(0,T) - 4k_B T \frac{\partial I_3(0,T,V_3)}{\partial V_3}\bigg|_{V_3=0}\right). \quad (3)$$

The noise $S_3(V,T) = 2\int_{-\infty}^{\infty} dt[I_3(t) - I_3][I_3(0) - I_3]$ is measured at D3. $\partial I_3(V,T,V_3)/\partial V_3|_{V_3=0}$ is measured with the voltage V_3 applied to S3 in addition to the voltage V at S1 and equals the correlation between the tunneling current $I(t)$ at QPC2 and the current from S3 to QPC2, according to the nonequilibrium fluctuation-dissipation theorem [42–44].

Main processes.—We discuss the origin of $\delta S < 0$. The tunneling current and its excess noise satisfy [45] $I = e^*(W_{2\to3} - W_{3\to2})$ and $\delta S = 2(e^*)^2(W_{2\to3} + W_{3\to2})$. $W_{2\to3}$ ($W_{3\to2}$) is the change, by the voltage V, in the rate for a particlelike (holelike) anyon to move from edge 2 to edge 3 at QPC2. Two types of processes, Poisson processes and TVBs, make the contribution $W_{i\to j}^{\mathrm{P}}$ and $W_{i\to j}^{\mathrm{TVB}}$, respectively, to $W_{i\to j}$,

$$W_{i\to j} \simeq W_{i\to j}^{\mathrm{P}} + W_{i\to j}^{\mathrm{TVB}} \quad \text{at } e^*V \gg k_B T. \quad (4)$$

$W_{i\to j}$ is computed in the Supplemental Material [41].

In the Poisson process [Fig. 1(b)] for $W_{2\to3}^{\mathrm{P}}$, a particlelike anyon, biased by the voltage V, moves from edge 1 to edge 3 through tunneling at QPC1 and QPC2. This leads to $W_{2\to3}^{\mathrm{P}} \propto \gamma_1^2\gamma_2^2 V^{4\nu-3}$, as the voltage-biased tunneling probability at QPCi and the current from S1 to QPC1 are proportional to $\gamma_i^2 V^{2\nu-2}$ and V, respectively. By contrast, $W_{3\to2}^{\mathrm{P}} = 0$, since tunneling of a holelike anyon from edge 2 to edge 3 is not induced by V.

Next, we consider the TVB for $W_{3\to2}^{\mathrm{TVB}}$. It is the interference of two subprocesses a_1 and a_2 [Fig. 1(c)]. In a_1 and a_2, a particlelike anyon, induced by the voltage V, moves from edge 1 to edge 2 via tunneling at QPC1 at time t_1 and then moves to D2. The operator for the QPC1 tunneling is $\mathcal{T}_{1\to2}(t_1) = \Psi_2^\dagger(0,t_1)\Psi_1(0,t_1)$. $\Psi_i^\dagger(x_i,t_1)$ creates an anyon at position x_i of edge i; QPC1 is located at $x_i = 0$. After (before) this anyon passes QPC2, a particle-hole pair is thermally excited at QPC2 at time t_2 (t_2') in the subprocess a_1 (a_2). Then the particlelike thermal anyon moves to D2 along edge 2, while the holelike one moves to D3 along edge 3. The excitation is described by the QPC2 tunneling operator $\mathcal{T}_{3\to2}(t) = \Psi_2^\dagger(d,t)\Psi_3(0,t)$ at $t = t_2$ (t_2') in a_1 (a_2); QPC2 is located at $x_2 = d$ ($x_3 = 0$) on edge 2 (edge 3).

To illustrate the nontrivial features (topological link by anyon braiding and the partner disconnected process) of the TVB for $W_{3\to2}^{\mathrm{TVB}}$, we consider the $V\to\infty$ limit where the voltage-biased particlelike anyon becomes a point particle [its spatial broadening $\hbar v/(e^*V) \to 0$; v is the anyon velocity]. In this limit, the correlator

$$C_{3\to2}^{\mathrm{TVB}} = \langle \mathcal{T}_{1\to2}^\dagger(t_1)\mathcal{T}_{3\to2}^\dagger(t_2')\mathcal{T}_{3\to2}(t_2)\mathcal{T}_{1\to2}(t_1)\rangle - \langle \mathcal{T}_{3\to2}^\dagger(t_2')\mathcal{T}_{3\to2}(t_2)\rangle\langle \mathcal{T}_{1\to2}^\dagger(t_1)\mathcal{T}_{1\to2}(t_1)\rangle \quad (5)$$

describes the TVB. $\langle\cdots\rangle$ is the ensemble average with the bare Hamiltonian [41] H_i of edge i.

The first term of Eq. (5) shows the interference between the subprocesses a_1 and a_2; $\mathcal{T}_{3\to2}(t_2)\mathcal{T}_{1\to2}(t_1)$ describes a_1, while $\mathcal{T}_{3\to2}(t_2')\mathcal{T}_{1\to2}(t_1)$ describes a_2. This term is factorized [41] into a subcorrelator for the voltage-biased anyon, another for the thermal anyons, and a phase factor $e^{i2\pi\nu}$ (Fig. 2),

$$\langle \mathcal{T}_{1\to2}^\dagger(t_1)\mathcal{T}_{3\to2}^\dagger(t_2')\mathcal{T}_{3\to2}(t_2)\mathcal{T}_{1\to2}(t_1)\rangle = e^{2i\pi\nu}\langle \mathcal{T}_{3\to2}^\dagger(t_2')\mathcal{T}_{3\to2}(t_2)\rangle\langle \mathcal{T}_{1\to2}^\dagger(t_1)\mathcal{T}_{1\to2}(t_1)\rangle, \quad (6)$$

by using the exchange rules of the fractional statistics $\Psi_i^\dagger(x)\Psi_i(y) = \Psi_i(y)\Psi_i^\dagger(x)e^{i\pi\nu \mathrm{sgn}(x-y)}$ and $\Psi_i^\dagger(x)\Psi_i^\dagger(y) = \Psi_i^\dagger(y)\Psi_i^\dagger(x)e^{-i\pi\nu \mathrm{sgn}(x-y)}$ (the rules between operators of different edges are constructed, using Klein factors [39,41]). The factor $e^{i2\pi\nu}$ is attributed to effective braiding of the thermal anyon around the voltage-biased anyon in the interference $a_2^* a_1$, depicted as the link of two loops in Fig. 2(b); the factorization is equivalent to untying the link. The solid blue loop corresponding to the subcorrelator $\langle \mathcal{T}_{3\to2}^\dagger(t_2')\mathcal{T}_{3\to2}(t_2)\rangle$ for the thermal anyons is formed, although $t_2 \neq t_2'$, with the help of the thermal length $\hbar v/(k_B T)$; $\langle \mathcal{T}_{3\to2}^\dagger(t_2')\mathcal{T}_{3\to2}(t_2)\rangle$ is nonvanishing for $|t_2 - t_2'| \lesssim \hbar/(k_B T)$. Similarly, at finite V, the dashed red loop representing $\langle \mathcal{T}_{1\to2}^\dagger(t_1)\mathcal{T}_{1\to2}(t_1)\rangle$ for the voltage-biased anyon is formed with $|t_1 - t_1'| \lesssim \hbar v/(e^* V)$, when the tunneling at QPC1 occurs at t_1' ($\neq t_1$) in a_2 as described by $\mathcal{T}_{1\to2}(t_1')$. In this case, the braiding occurs for $t_2' < t_1 + d/v < t_2$ and $t_2' < t_1' + d/v < t_2$.

The effective braiding ($e^{2i\pi\nu}$) is decomposed into two events of anyon exchange. One exchange ($e^{i\pi\nu}$) occurs in the subprocess a_1 when the thermal anyon is excited on edge 2 at QPC2 [Fig. 2(a)]. It happens such that the thermal anyon effectively moves from the right side of the voltage-biased anyon to the left on edge 2 (see Supplemental Material [41]). The other ($e^{i\pi\nu}$) occurs in the interference $a_2^* a_1$. The voltage-biased anyon of a_2 moves back to QPC1, passing the thermal anyon of a_1 [the top dashed arrow in Fig. 2(b)].

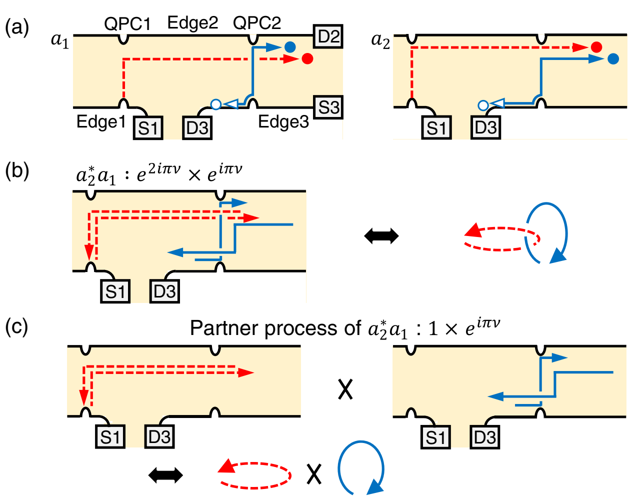

FIG. 2. TVB interference for $W_{3\to2}^{\mathrm{TVB}}$. (a) Its subprocesses a_1 and a_2 [identical to those in Fig. 1(c)] have the trajectory (dashed red arrows) of a voltage-biased anyon (red filled circles) and that (solid blue) of a thermal pair excitation of a particlelike anyon (blue filled) and a holelike anyon (blue empty). Two trajectories are drawn to cross when the corresponding operators are non-commutative due to the fractional statistics. The crossing is time ordered such that the later trajectory is drawn on top of the earlier one. (b) TVB interference $a_2^* a_1$ between a_1 and a_2. The trajectories of a_2^*, the complex conjugation of a_2, are drawn on top of those of a_1. The loop formed by the dashed red trajectories is topologically linked with that by the solid blue ones, implying effective braiding of the thermal anyon around the voltage-biased anyon. The braiding phase factor is $e^{2i\pi\nu}$. (c) In the partner disconnected process of $a_2^* a_1$, the two loops are unlinked, showing no braiding. $a_2^* a_1$ and its partner have a common phase factor $e^{i\pi\nu}$ due to an exchange of a thermal anyon of a_1 and another of a_2 (the crossing of solid blue trajectories).

We call the first term of Eq. (5) a TVB since the trajectory (dashed red loop) of the voltage-biased anyon and that (solid blue loop) of the thermal anyon are disconnected from each other in the conventional sense but topologically linked [35] by the braiding. The TVB is accompanied by a partner *disconnected* process [Fig. 2(c)] that gives the second term of Eq. (5) and has the same subprocesses as the TVB except the braiding. The TVB and its partner disconnected process [or the correlator in Eq. (5)] appear in our calculation [41] of $W_{i\to j}$. The pairwise appearance is understood by considering electrons at $\nu = 1$. For the electrons, the TVB is described by a disconnected Feynman diagram as the braiding link has no meaning, $e^{2i\pi\nu} = 1$. Then it must be accompanied and exactly canceled [leading to $C_{3\to2}^{\mathrm{TVB}} = 0$; cf., Eqs. (5) and (6)] by the partner disconnected diagram, following the linked cluster theorem [34]; the second term of Eq. (5) has the minus sign for the cancellation. Mathematically, the partner diagram appears due in part to the partition function of a Green's function in its perturbation expansion; hence it does not have the braiding link. For the anyons, the cancellation is partial, because of the braiding.

The common factor of the two terms of Eq. (5) is further factorized with a correlator $D_i(x,t,t') = \langle \Psi_i^\dagger(x,t)\Psi_i(x,t')\rangle$ of each edge i,

$$\langle \mathcal{T}_{3\to2}^\dagger(t_2')\mathcal{T}_{3\to2}(t_2)\rangle\langle \mathcal{T}_{1\to2}^\dagger(t_1)\mathcal{T}_{1\to2}(t_1)\rangle = e^{i\pi\nu} D_2(d,t_2,t_2')D_3(0,t_2,t_2')D_1(0,t_1,t_1)D_2(0,t_1,t_1). \tag{7}$$

The factor $e^{i\pi\nu}$ comes from exchange of a thermal anyon of a_1 and another of a_2 [Figs. 2(b) and 2(c)].

The TVB and its partner disconnected process give

$$W_{3\to2}^{\mathrm{TVB}} \propto \gamma_1^2\gamma_2^2 V^{2\nu-1}T^{2\nu-2}\mathrm{Re}[e^{i\pi\nu}(e^{2i\pi\nu}-1)], \tag{8}$$

as the thermal (voltage-biased) tunneling probability at QPC2 (QPC1) is proportional to $\gamma_2^2 T^{2\nu-2}$ ($\gamma_1^2 V^{2\nu-2}$), while the current from S1 to QPC1 is proportional to V. The phase factors come from $\mathrm{Re}[C_{3\to2}^{\mathrm{TVB}}] \propto \mathrm{Re}[e^{i\pi\nu}(e^{2i\pi\nu}-1)]$ in Eqs. (5)–(7). $\mathrm{Re}[\cdots]$ is taken, considering $[C_{3\to2}^{\mathrm{TVB}}]^*$.

There is a TVB process for $W_{2\to3}^{\mathrm{TVB}}$. $W_{2\to3}^{\mathrm{TVB}}$ is negligibly small at $e^*V \gg k_B T$ [46].

We now compute $\delta S/I$. At $e^*V \gg k_B T$ and $\nu = 1/(2n+1) < 1$, the TVB for $W_{3\to2}^{\mathrm{TVB}}$ and its partner disconnected process dominate over the Poisson process for $W^{\rm P}_{2\to3}$, $W^{\rm TVB}_{3\to2} \gg W^{\rm P}_{2\to3}$; cf., Eq. (8) and $W^{\rm P}_{2\to3} \propto \gamma_1^2\gamma_2^2 V^{4\nu-3}$. Hence, they determine the current and the excess noise, $I = -e^* W^{\rm TVB}_{3\to2}$ and $\delta S = 2(e^*)^2 W^{\rm TVB}_{3\to2}$, leading to Eqs. (1) and (2). We emphasize that the ratio $\delta S/I$ has the negative universal value of $-2e^*$. This originates from the TVB for $W^{\rm TVB}_{3\to2}$ and its partner disconnected process and, equivalently, from the anyon braiding. It is nontrivial that the disconnected process contributes to the observables I and δS; for electrons or bosons, disconnected Feynman diagrams never contribute to observables [34].

The above findings are confirmed by numerically computing δS (see Supplemental Material [41]). For $\nu = 1/3$, δS approaches to $-2e^*I$ such that $\delta S = -1.8e^*I$ at $V = 60\ \mu$V at 50 mK and $-1.99e^*I$ at 80 μV at 50 mK.

Discussion.—The negative excess noise $\delta S < 0$ results from the TVB process for $W^{\rm TVB}_{3\to2}$. It is interpreted as follows. At $V = 0$, tunneling of a particlelike or holelike anyon between edge 2 and edge 3 is thermally induced at QPC2, causing the thermal noise $S(0, T)$. Among those tunneling events, thermal tunneling of a holelike anyon from edge 2 to edge 3 is weakened by a voltage-biased particlelike anyon injected from edge 1 to edge 2, when the voltage V is applied to edge 1. The weakening is due to the effective braiding of the thermal anyon around the voltage-biased anyon, which results in the partial cancellation between the TVB and its partner disconnected process, $W^{\rm TVB}_{3\to2} \propto {\rm Re}[e^{i\pi\nu}(e^{2i\pi\nu} - 1)] < 0$. The weakening leads to the current $I > 0$ and the reduction of the noise $S(V, T)$ below $S(0, T)$. Note that $\delta S < 0$ at any V, although both the Poisson process and the TVB (and its partner) contribute to δS at $e^*V \lesssim k_B T$.

By contrast, for electrons at $\nu = 1$, the Poisson process determines $I = eW^{\rm P}_{2\to3}$ and $\delta S = 2e^2 W^{\rm P}_{2\to3}$, leading to $\delta S = 2eI > 0$ at $e^*V \gg k_B T$. There is no topological link by the braiding ($e^{2i\pi\nu} = 1$), and the TVB becomes a disconnected process and fully canceled by its partner disconnected diagram, $W^{\rm TVB}_{i\to j} = 0$. This is why the excess noise $\delta S = 2eI$ of the electrons cannot be extrapolated from Eq. (1) with $e^* \to e$.

Measurement of δS is feasible, as the setup was experimentally studied in other contexts [30–32]: typically, the tunneling probability of QPC1 and QPC2 is set to be 0.2, to have anyon tunneling [24]. We estimate $I \sim 50$ pA and $\delta S \sim 2.7 \times 10^{-30}\ {\rm A^2/Hz}$ at 100 μV and $\nu = 1/3$, which is detectable [30,47]. When δS is measured by using Eq. (3), one has to experimentally determine temperature T. The determination accuracy is within ± 3 mK [47]. Then, it is possible to obtain $\delta S = -2e^*I(1 \pm 0.2)$ at 50 mK, $V = 80\ \mu$V, and $\nu = 1/3$.

Our study is generalized to edges with multiple channels or reconstruction (see Supplemental Material [41]). For example, at a filling factor of 4/3 or 7/3 [18,48], the inner fractional edge channel corresponding to $\nu = 1/3$ interacts with copropagating outer channels and is weakly backscattered at the QPCs. In this case, δS is still negative. On the other hand, when the $\nu = 1/3$ edge channel interacts with an unexpected counterpropagating mode [49] due to edge reconstruction, δS is negative only when the interaction is sufficiently weak [25,50]. The outer channels at a filling factor of 4/3 or 7/3 are helpful in this case, since they can screen the edge reconstruction. In the above cases of multiple channels or edge reconstruction, detection of $\delta S < 0$ may imply the fractional statistics of the quasiparticles deviating from Laughlin anyons due to the interchannel interactions. The quasiparticles become closer to Laughlin anyons for weaker interactions.

In summary, we predict the negative excess autocorrelation noise $\delta S < 0$, a signature of the Abelian fractional statistics or the new process (TVB) not existing with fermions or bosons. It is unusual that the excess autocorrelation noise of electrical tunneling current is negative [21,51].

We suggest that autocorrelation noise can provide signatures [52,53] of identical-particle statistics. This is different from the conventional approach [54–56] of detecting particle bunching or antibunching with Hanbury Brown–Twiss cross-correlations. It is unnatural to interpret the negative excess autocorrelation noise as deviation (anyonic partial bunching [5–9]) from fermionic antibunching and bosonic bunching, because it originates from the TVB having no counterpart in fermions or bosons.

We thank Hyungkook Choi, Sang-Jun Choi, Yunchul Chung, Sourin Das, Dmitri Feldman, Bertrand Halperin, Charles Kane, and Bernd Rosenow for valuable discussions, and acknowledge the support by Korea NRF (SRC Center for Quantum Coherence in Condensed Matter, Grant No. 2016R1A5A1008184).

*hssim@kaist.ac.kr

[1] J. M. Leinaas and J. Myrheim, On the theory of identical particles, Nuovo Cimento B 37, 1 (1977).
[2] D. Arovas, J. R. Schrieffer, and F. Wilczek, Fractional Statistics and the Quantum Hall Effect, Phys. Rev. Lett. 53, 722 (1984).
[3] A. Stern, Anyons and the quantum Hall effect–A pedagogical review, Ann. Phys. (Amsterdam) 323, 204 (2008).
[4] C. de C. Chamon, D. E. Freed, S. A. Kivelson, S. L. Sondhi, and X. G. Wen, Two point-contact interferometer for quantum Hall systems, Phys. Rev. B 55, 2331 (1997).
[5] I. Safi, P. Devillard, and T. Martin, Partition Noise and Statistics in the Fractional Quantum Hall Effect, Phys. Rev. Lett. 86, 4628 (2001).
[6] S. Vishveshwara, Revisiting the Hanbury Brown–Twiss Setup for Fractional Statistics, Phys. Rev. Lett. 91, 196803 (2003).
[7] E.-A. Kim, M. J. Lawler, S. Vishveshwara, and E. Fradkin, Signatures of Fractional Statistics in Noise Experiments in Quantum Hall Fluids, Phys. Rev. Lett. 95, 176402 (2005).

[8] G. Campagnano, O. Zilberberg, I. V. Gornyi, D. E. Feldman, A. C. Potter, and Y. Gefen, Hanbury Brown–Twiss Interference of Anyons, Phys. Rev. Lett. **109**, 106802 (2012).

[9] B. Rosenow, I. P. Levkivskyi, and B. I. Halperin, Current Correlations from a Mesoscopic Anyon Collider, Phys. Rev. Lett. **116**, 156802 (2016).

[10] C. L. Kane, Telegraph Noise and Fractional Statistics in the Quantum Hall Effect, Phys. Rev. Lett. **90**, 226802 (2003).

[11] K. T. Law and D. E. Feldman, Electronic Mach-Zehnder interferometer as a tool to probe fractional statistics, Phys. Rev. B **74**, 045319 (2006).

[12] E. Grosfeld, S. H. Simon, and A. Stern, Switching Noise as a Probe of Statistics in the Fractional Quantum Hall Effect, Phys. Rev. Lett. **96**, 226803 (2006).

[13] F. E. Camino, W. Zhou, and V. J. Goldman, $e/3$ Laughlin Quasiparticle Primary-Filling $= 1/3$ Interferometer, Phys. Rev. Lett. **98**, 076805 (2007).

[14] D. E. Feldman, Y. Gefen, A. Kitaev, K. T. Law, and A. Stern, Shot noise in an anyonic Mach-Zehnder interferometer, Phys. Rev. B **76**, 085333 (2007).

[15] R. L. Willett, L. N. Pfeiffer, and K. W. West, Measurement of filling factor 5/2 quasiparticle interference with observation of charge $e/4$ and $e/2$ period oscillations, Proc. Natl. Acad. Sci. U.S.A. **106**, 8853 (2009).

[16] N. Ofek, A. Bid, M. Heiblum, A. Stern, V. Umansky, and D. Mahalu, Role of interactions in an electronic Fabry Perot interferometer operating in the quantum Hall effect regime, Proc. Natl. Acad. Sci. U.S.A. **107**, 5276 (2010).

[17] B. Halperin, A. Stern, I. Neder, and B. Rosenow, Theory of the Fabry-Perot quantum Hall interferometer, Phys. Rev. B **83**, 155440 (2011).

[18] S. An, P. Jiang, H. Choi, W. Kang, S. H. Simon, L. N. Pfeiffer, K. W. West, and K. W. Baldwin, Braiding of Abelian and non-Abelian anyons in the fractional quantum Hall effect, arXiv:1112.3400.

[19] B. Rosenow and S. H. Simon, Telegraph noise and the Fabry-Perot quantum Hall interferometer, Phys. Rev. B **85**, 201302(R) (2012).

[20] D. T. McClure, W. Chang, C. M. Marcus, L. N. Pfeiffer, and K. W. West, Fabry-Perot Interferometry with Fractional Charges, Phys. Rev. Lett. **108**, 256804 (2012).

[21] Ya. M. Blanter and M. Büttiker, Shot noise in mesoscopic conductors, Phys. Rep. **336**, 1 (2000).

[22] M. Reznikov, M. Heiblum, Hadas Shtrikman, and D. Mahalu, Temporal Correlation of Electrons: Suppression of Shot Noise in a Ballistic Quantum Point Contact, Phys. Rev. Lett. **75**, 3340 (1995).

[23] C. L. Kane and Matthew P. A. Fisher, Nonequilibrium Noise and Fractional Charge in the Quantum Hall Effect, Phys. Rev. Lett. **72**, 724 (1994).

[24] R. de-Picciotto, M. Reznikov, M. Heiblum, V. Umansky, G. Bunin, and D. Mahalu, Direct observation of a fractional charge, Nature (London) **389**, 162 (1997).

[25] L. Saminadayar, D. C. Glattli, Y. Jin, and B. Etienne, Observation of the $e/3$ Fractionally Charged Laughlin Quasiparticle, Phys. Rev. Lett. **79**, 2526 (1997).

[26] M. Reznikov, R. de Picciotto, T. G. Griffiths, M. Heiblum, and V. Umansky, Observation of quasiparticles with one-fifth of an electron's charge, Nature (London) **399**, 238 (1999).

[27] T. G. Griffiths, E. Comforti, M. Heiblum, A. Stern, and V. Umansky, Evolution of Quasiparticle Charge in the Fractional Quantum Hall Regime, Phys. Rev. Lett. **85**, 3918 (2000).

[28] M. Dolev, M. Heiblum, V. Umansky, A. Stern, and D. Mahalu, Observation of a quarter of an electron charge at the $\nu = 5/2$ quantum Hall state, Nature (London) **452**, 829 (2008).

[29] V. J. Goldman and B. Su, Resonant tunneling in the quantum Hall regime: Measurement of fractional charge, Science **267**, 1010 (1995).

[30] E. Comforti, Y. C. Chung, M. Heiblum, V. Umansky, and D. Mahalu, Bunching of fractionally-charged quasiparticles tunneling through high potential barriers, Nature (London) **416**, 515 (2002).

[31] E. Comforti, Y. C. Chung, M. Heiblum, and V. Umansky, Multiple Scattering of Fractionally-Charged Quasiparticles, Phys. Rev. Lett. **89**, 066803 (2002).

[32] Y. C. Chung, M. Heiblum, Y. Oreg, V. Umansky, and D. Mahalu, Anomalous chiral Luttinger liquid behavior of diluted fractionally charged quasiparticles, Phys. Rev. B **67**, 201104(R) (2003).

[33] There is a theoretical work on the effect of dilute anyon injection on tunneling charges at a QPC in a FQH setup where the QPC is tuned from weak to strong backscattering regimes. See C. L. Kane and M. P. A. Fisher, Shot noise and the transmission of dilute Laughlin quasiparticles, Phys. Rev. B **67**, 045307 (2003). This work does not discuss any effect of the anyon fractional statistics. By contrast, in our Letter, we propose to use dilute anyon injection for observing the fractional statistics, focusing on the weak backscattering regime of QPCs.

[34] For bosons and fermions, disconnected diagrams never contribute to observables. See, e.g., A. L. Fetter and J. D. Walecka, *Quantum Theory of Many-Particle Systems* (McGraw-Hill, New York, 1971).

[35] Disconnected diagrams but linked by braiding appear in the algebraic theory of anyons. See, e.g., J. Preskill, *Lecture Notes for Physics 219: Quantum Computation* (California Institute of Technology, Pasadena, CA, 1998); See also A. Kitaev, Anyons in an exactly solved model and beyond, Ann. Phys. (Amsterdam) **321**, 2 (2006).

[36] C. Han, J. Park, Y. Gefen, and H.-S. Sim, Topological vacuum bubbles by anyon braiding, Nat. Commun. **7**, 11131 (2016). While this previous work studied the transport mechanism of a Fabry-Perot interference current in a three-QPC setup, the present Letter predicts a new mechanism of shot noise at a single QPC in the simpler two-QPC setup.

[37] X. G. Wen, Chiral Luttinger liquid and the edge excitations in the fractional quantum Hall states, Phys. Rev. B **41**, 12838 (1990).

[38] J. von Delft and H. Schoeller, Bosonization for beginners—Refermionization for experts, Ann. Phys. (Berlin) **7**, 225 (1998).

[39] R. Guyon, P. Devillard, T. Martin, and I. Safi, Klein factors in multiple fractional quantum Hall edge tunneling, Phys. Rev. B **65**, 153304 (2002).

[40] Note that the correction of order $O(T/V)$ to Eq. (1) is found as $\delta S/I = -2e^*\{1 + [4\nu(1-2\nu)/\sin 2\pi\nu][\pi k_B T/e^* V]\}$. It

occurs due to the spatial broadening $\hbar v/(e^* V)$ of the voltage-biased anyon that leads to imperfection of the effective braiding.

[41] See Supplemental Material at http://link.aps.org/supplemental/10.1103/PhysRevLett.123.016803 for the Hamiltonian and operators of the setup, Klein factors, expression of $f(\nu)$, derivation of Eqs. (3) and (6), effective braiding, detailed computation of $W_{i\to j}$, correction of order $O(T/V)$ to Eq. (1), and effect of multiple edge channels and edge reconstruction.

[42] C. Wang and D. E. Feldman, Fluctuation-dissipation theorem for chiral systems in nonequilibrium steady states, Phys. Rev. B **84**, 235315 (2011).

[43] C. Wang and D. E. Feldman, Chirality, Causality, and Fluctuation-Dissipation Theorems in Nonequilibrium Steady States, Phys. Rev. Lett. **110**, 030602 (2013).

[44] O. Smits, J. K. Slingerland, and S. H. Simon, Non-equilibrium noise in the (non-)Abelian fractional quantum Hall effect, arXiv:1401.4581.

[45] D. E. Feldman and M. Heiblum, Why a noninteracting model works for shot noise in fractional charge experiments, Phys. Rev. B **95**, 115308 (2017).

[46] The TVB process for $W^{\mathrm{TVB}}_{2\to 3}$ is identical to that of $W^{\mathrm{TVB}}_{3\to 2}$, except that its thermal anyons move in the opposite direction to those of $W^{\mathrm{TVB}}_{3\to 2}$. $W^{\mathrm{TVB}}_{2\to 3}$ has the same expression as $W^{\mathrm{TVB}}_{3\to 2}$ in Eq. (8), but with the replacement of $e^{2i\pi\nu} \to e^{-2i\pi\nu}$.

[47] Current $\gtrsim 0.5$ pA and noise $\gtrsim 10^{-30}$ A^2/Hz are well detectable. Y. C. Chung and H.-K. Choi, (private communication).

[48] S. Baer, C. Rössler, T. Ihn, K. Ensslin, C. Reichl, and W. Wegscheider, Experimental probe of topological orders and edge excitations in the second Landau Level, Phys. Rev. B **90**, 075403 (2014).

[49] B. Rosenow and B. I. Halperin, Nonuniversal Behavior of Scattering between Fractional Quantum Hall Edges, Phys. Rev. Lett. **88**, 096404 (2002).

[50] S. Roddaro, V. Pellegrini, and F. Beltram, Nonlinear Quasiparticle Tunneling between Fractional Quantum Hall Edges, Phys. Rev. Lett. **90**, 046805 (2003).

[51] For noninteracting electrons, a negative excess noise can appear, not originating from the fermionic statistics, in a certain situation irrelevant to our case. See, e.g., G. B. Lesovik and R. Loosen, Negative excess noise in quantum conductors, Z. Phys. B **91**, 531 (1993); See also F. Dolcini and H. Grabert, Tuning excess noise by Aharonov-Bohm interferometry, Chem. Phys. **375**, 291 (2010).

[52] Negative excess noise can occur due to the bosonic statistics. See, e.g., M. Büttiker, Scattering theory of current and intensity noise correlations in conductors and wave guides, Phys. Rev. B **46**, 12485 (1992); See also J. H. Davies, P. Hyldgaard, S. Hershfield, and J. W. Wilkins, Classical theory for shot noise in resonant tunneling, Phys. Rev. B **46**, 9620 (1992).

[53] Generalization of our results to non-Abelian statistics is in progress. B. Lee, C. Han, and H.-S. Sim (in preparation).

[54] M. Henny, S. Oberholzer, C. Strunk, T. Heinzel, K. Ensslin, M. Holland, and C. Schönenberger, The fermionic Hanbury Brown and Twiss Experiment, Science **284**, 296 (1999).

[55] W. D. Oliver, J. Kim, R. C. Liu, and Y. Yamamoto, Hanbury Brown and Twiss-Type Experiment with electrons, Science **284**, 299 (1999).

[56] T. Jeltes, J. M. McNamara, W. Hogervorst, W. Vassen, V. Krachmalnicoff, M. Schellekens, A. Perrin, H. Chang, D. Boiron, A. Aspect, and C. I. Westbrook, Comparison of the Hanbury Brown-Twiss effect for bosons and fermions, Nature (London) **445**, 402 (2007).